Dynamic change in the surface and layer structures during epitaxial growth of Si on a Si(111)-7×7 surface

Y. Fukaya, Y. Shigeta,* and K. Maki
Faculty of Science & Graduate School of Integrated Science, Yokohama City University, Seto 22-2, Kanazawa-ku, Yokohama 236-0027, Japan
(Received 12 July 1999)

In order to investigate the dynamic process during growth of a Si layer on the Si(111)-7×7 surface held at 380 °C, the rocking curve of reflection high-energy electron diffraction (RHEED) is continuously measured at 0.5° to 6° at intervals of 0.05° to the glancing angle of the incident electron beam which takes 18 sec. At the initial growth stage, the multilayer islands are grown on the native 7×7 surface with broader Bragg peaks in the rocking curve than those from the native surface. The sharpness of the Bragg peak is subsequently recovered after the thickness of the Si layer reaches 3 BL (1 BL=0.31 nm), at which the growth transforms to layer-by-layer growth. The comparison of the measured rocking curve with the calculated one based on the dynamical theory of RHEED intensity is also performed by optimizing each atomic position in the growing layer so as to minimize the difference between both curves. The space of the double layer of the (111) plane in the multilayer islands expands and is restored to the normal spacing after the growth mode transforms to the layer-by-layer mode. The broadening of the Bragg peaks at the initial growth stage relates to the rearrangement process of a stacking-fault layer in the 7×7 structure on the substrate surface.

I. INTRODUCTION

We have studied the homoepitaxial growth process of Si layers on the 7×7 superlattice surface of the Si(111) substrate held at temperatures below 400 °C with low-energy electron diffraction[1] and scanning tunneling microscopy (STM) (Refs. 2–5) in terms of clarifying the growth mechanism. Since the substrate temperature is relatively low to a normal epitaxial condition, some works have been published with a title containing ''*low-temperature epitaxy*.''[6,7] Under the low-temperature epitaxy condition, the initial growth progresses by a three-dimensional nucleation and growth process until the native 7×7 superlattice surface of the Si(111) substrate is completely covered with a Si layer.[2,4] The reason why the lateral growth of two-dimensional (2D) islands is restricted, is the necessity for rearrangement of atoms in the stable 7×7 dimer-adatom-stacking-fault (DAS) structure[8] to the Si bulk structure when the 7×7 DAS structure is covered with the growing layer. On the other hand, the lateral growth of 2D islands on the growing layer is not restricted and follows the layer-by-layer growth, because the surface on the growing layer is composed of small domains of the metastable surface structures, which are easy to be rearranged. The transformation of the growth mode was clearly shown by a sequence of STM images after quenching at each growth stage.

We considered that the surface morphology *during growth* is different from *after growth*. In order to confirm the view, we constructed the system for *in situ* observation of the rocking curve of reflection high-energy electron diffraction (RHEED).[9] In the previous study, we measured RHEED rocking curves continuously during growth at a temperature (T_s) of 250 °C. We showed that the presence of a two-dimensional atomic gas on the surface during growth is essential by comparison with the calculated intensity.[10] The morphology change during growth at an elevated temperature is very interesting, because the abnormal behavior in the intensity oscillation of the RHEED,[11] which is related to the growth of three-dimensional (3D) islands at the initial growth stage, increases remarkably at $T_s = 380$ °C.[4]

In this study, we will show the RHEED rocking curves measured *during growth* of a Si layer on the Si(111)-7×7 surface held at 380 °C. These curves are compared with the calculated intensity under one-beam condition in RHEED dynamical theory developed by Ichimiya.[12,13] We propose a structural model estimated by optimizing each atomic position in the growing layer so as to minimize the difference between both curves by using the Levenberg–Marquardt method.[14,15]

II. EXPERIMENTAL PROCEDURE

The substrates used in this study were Si bars ($5 \times 25 \times 0.4\,\mathrm{mm}^3$) cut from a mirror-polished commercial *n*-type Si(111) wafer (1.0–4.0 Ω cm). The substrate was heated by a direct current flow with the following steps: (1) heated up to 1150 °C for 3 h and then (2) flashed at 1200 °C for a few minutes at a pressure below 5×10^{-8} Pa. We deposited the Si layer on the Si(111) substrate held at 380 °C by an electron beam evaporator. The deposition rate $\boldsymbol{r}$ was monitored with a quartz oscillator and kept $\boldsymbol{r} = 0.27$ BL/min, where 1 BL means 0.31 nm in mean thickness.

We used a homebuilt RHEED apparatus equipped with a magnetic deflector composed of two pairs of magnetic coils as reported previously.[9] We controlled the glancing angle (θ) of the incident high-energy electron beam, which was accelerated at 10 kV, from 0.5° to 6° using steps of 0.05° for 18 sec. We chose the azimuthal angle of the incident beam at 7.5° from the $[11\bar{2}]$ direction in order to avoid the diffraction condition, under which the simultaneous reflections for

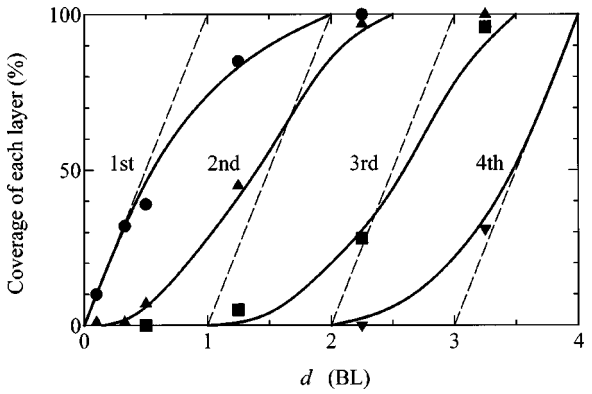

FIG. 1. Coverage occupied by each layer as a function of mean thickness, *d*. The closed circle, triangle, square, and reverse triangle show the coverage of the first, second, third, and fourth layer, respectively. Each value was estimated from the STM images in Ref. 4.

many lattice planes are formed, in particular, the diffracted waves propagate parallel to the surface. Such a diffraction condition is called ''under the one-beam condition.'' [16] Each RHEED pattern recorded at every 0.05° step in θ was imaged with a TV camera and stored on a laser video disk during growth. We obtained the integrated intensity of each spot on the (00) rod through a flame memory and plotted a rocking curve.

III. RHEED INTENSITY CALCULATION

We calculated the RHEED intensity according to dynamical theory[12,13] under the one-beam condition. The reliability of the RHEED intensity calculated by using a model potential was verified to compare with the experimental result. The reliability factor (R) was defined as,

$$R=\frac{\sqrt{\Sigma(\alpha I_\theta^{\mathrm{cal}}-I_\theta^{\mathrm{mea}})^2}}{\Sigma I_\theta^{\mathrm{mea}}}\times 100\,[\%],$$

$$\alpha=\frac{\Sigma I_\theta^{\mathrm{mea}}}{\Sigma I_\theta^{\mathrm{cal}}},$$

where I_θ^{mea} and I_θ^{cal} were the measured and calculated intensity at the glancing angle, θ, respectively. All data measured at every θ (about 110 points) were included to calculate the R factor.

The potential in this calculation was estimated from the surface morphology, which was determined by the coverage of each layer and the structure model on the surface of the growing layer.[9,10] The coverage of each layer was determined from the STM images measured in the previous study.[4] Figure 1 shows the relationship between the coverage and the mean thickness (d) at $T_s=380\,^\circ$C. For example, we can determine that each coverage of the first, second, and third layer at $d=1.25$ BL is 85%, 45%, and 5%, respectively.

We assume that the atoms in the growing layer are positioned at the same positions as the substrate surface, on which the 7×7 DAS structure is formed. In the one-beam calculation, the potential for the structure model is determined by the normal component (Z_i) of atomic positions and the number density (ρ) of atoms at Z_i in the 7×7 unit cell (the so-called ''one-beam potential'').[9,10] The wave field is influenced by the three-dimensional potential within the coherent length of primary electrons, which is about a few hundred nm at $\theta<6°$. The coherent length is much larger than the island size and mean distance between islands. Under the one-beam condition, the effect of the simultaneous reflections is suppressed, so that the periodicity of the potential parallel to the surface can be ignored. The one-beam potential depends only on the atomic displacements normal to the surface (the zeroth term of Fourier series of the crystal potential parallel to the surface).

The STM observation shows that the 5×5 and 9×9 DAS structures coexist with the 7×7 DAS structure on the growing surface.[2,4] However, we assume that the structure on the surface of growing layer is the same as the 7×7 DAS structure, because the one-beam potentials of 5×5 and 9×9 DAS structures are very close to that of the 7×7 DAS structure. The difference among the calculated rocking curves for the 7×7, 5×5, and 9×9 DAS structures is very small, and the R factors of the 5×5 and 9×9 structures to the 7×7 structure are smaller than 1%, which is much smaller than the experimental error of 3%.

IV. RESULTS AND DISCUSSION

Figure 2 shows a sequence of measured RHEED rocking curves during growth up to $d=4$ BL. We measured 12 RHEED rocking curves for the growth of 1 BL. The mean thickness d is labeled on the right-hand side of each panel. The features of the rocking curves are as follows.

(1) The peak at $\theta=1.3°$ gradually shifts to lower angle and the peak height decreases with growth. The peak disappears when d reaches approximately 2 BL.

(2) The peak at $\theta=1.8°$ appears at $d\approx0.4$ BL, and gradually shifts to lower angle with growth.

(3) In further growth, these peaks seems to construct one peak at $\theta=1.3°$ with growth of $d=3$ BL.

(4) The 333, 444, and 555 Bragg peaks become broader with growth, and subsequently become sharp when d approaches 3 BL. The growth stage showing the broadening of the Bragg peaks corresponds to the growth period of 3D islands on the substrate (see Fig. 1). For growth over 3 BL, the growth mode transforms from 3D island growth to the layer-by-layer growth[4] and the rocking curve shows a regular oscillation with a period of 1 BL.

To highlight intensity changes with growth, we plot the intensity at arbitrary glancing angles in Fig. 2 as a function of deposition time, $\boldsymbol{t}_d$, as shown in Fig. 3. The mean thickness corresponding to $\boldsymbol{t}_d$ during growth is also indicated on the top of Fig. 3. The intensity clearly displays a regular oscillation after the growth of 3 BL, which relates to the start of layer-by-layer growth, instead of 3D island growth,[1,4] where the phase of the regular oscillations also changes with θ.

Figure 4 shows the calculated rocking curves picked out every 0.5 BL for $d<4$ BL, in which the solid and dotted lines indicate calculated and measured curves, respectively. We see that the difference in the peak position between both curves is very large at a low glancing angle ($<2.5°$), except for the curves at $d=0$ BL and $d=4$ BL. We also note that the width of Bragg peaks in the measured curves is much

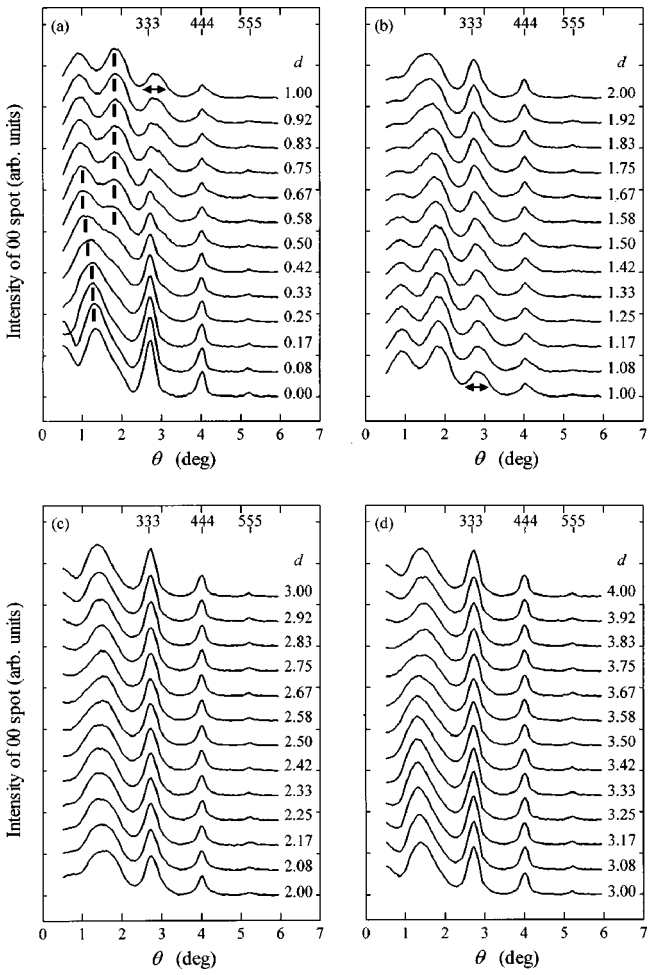

FIG. 2. RHEED rocking curves of the Si/Si(111) surface during growth at $Ts=380\,^{\circ}\mathrm{C}$ and $r=0.27$ BL/min: (a) $d=0-1$ BL, (b) $d=1-2$ BL, (c) $d=2-3$ BL, and (d) $d=3-4$ BL. The accelerated voltage of incident electrons is 10 kV and the azimuth angle deviates 7.5° from the $[11\bar{2}]$ direction. The mean thickness d is labeled on the right-hand side.

wider than that in the calculated curves at $0.5<d<2.0$ BL. Although we have tried to calculate rocking curves considering the two-dimensional atomic gas, we cannot explain the large difference at low glancing angle and the broadening of Bragg peaks at the initial growth stage. As a possible model to explain the broadening of Bragg peaks, we considered the deviation of atomic position from that of DAS structure on the growing layer. Thus we tried to optimize atomic positions in the growing layer by *keeping the coverage of each layer* a certain value so as to fit the measured curve. We performed the optimization of the atomic positions of all layers by using the Levenberg–Marquardt method.[14,15]

Figure 5 shows the calculated rocking curves after the optimization of the atomic positions in the DAS structure, in which the solid lines indicate the calculated curves and the dotted lines are the measured curves. The intensity at $\theta<2.5°$ for $d=0.5-3.5$ BL and the width of the Bragg peaks are improved, and the calculated curves represent the characteristics of the measured curves during growth. For all calculated curves, the R factor judging the goodness of the fit is smaller than 3%. The optimized atomic positions at each growth stage are shown in Figs. 6. A model of the first growing layer showing the notation of each atomic position is drawn in Fig. 6(a). The numbers labeled in the figure correspond to each atom classified into nine groups according to their Z coordinate (see Ref. 9). In Fig. 6(b), nine solid lines show the change of each atomic position with increasing d, and the dotted lines indicate the atomic position before the optimization, i.e., corresponding to atomic positions of the

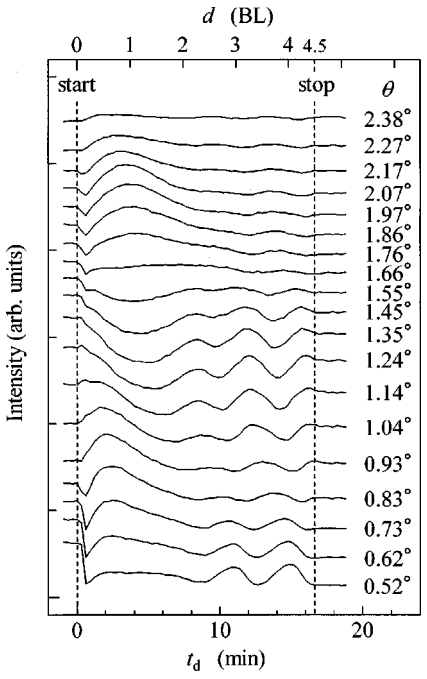

FIG. 3. Intensity change of 00 spot at each glancing angle θ as a function of the deposition time t_d. The mean thickness corresponding to t_d during growth is also indicated on the top of the figure.

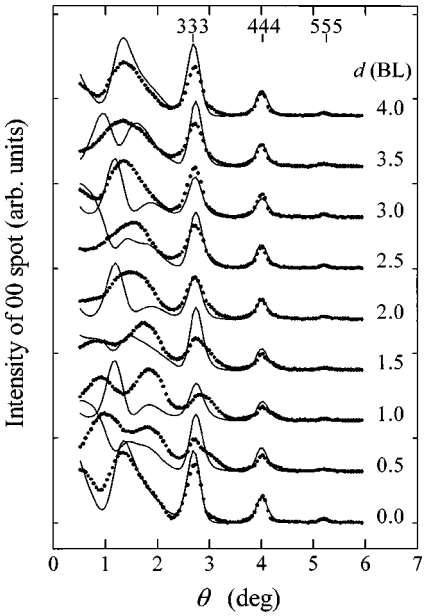

FIG. 4. Calculated rocking curves determined from the surface morphology which is estimated from the coverage of each layer in Fig. 1 and the DAS structure at *the same atomic position as the substrate*. Nine rocking curves are selected from the growth up to 4 BL. The measured rocking curves are also plotted by dotted lines.

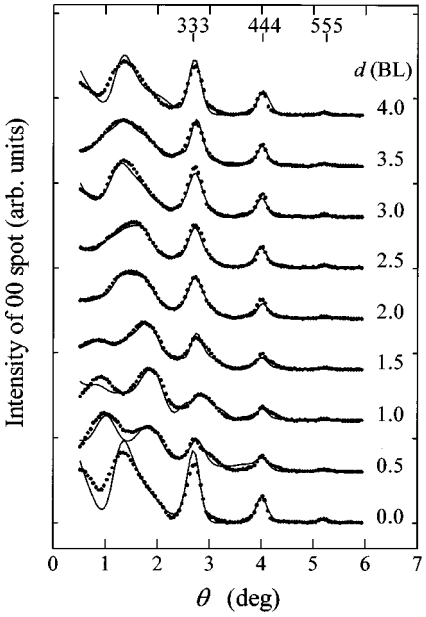

FIG. 5. Calculated rocking curves determined from the surface morphology when the atomic positions in DAS structure are optimized. Each calculated rocking curve is consistent with the measured curves plotted by dotted lines.

7×7 DAS structure. A thick line in the lower part of Fig. 6(b) shows the change in the unoccupied area with the second layer on the first layer, i.e., the naked area. We note that the change of atomic positions in each layer must have a great effect on the calculated intensity, when the naked area becomes maximum [i.e., at $d=1$ BL in Fig. 6(b)]. From this result, we note that the space between the upper layer (labeled 3) and the lower layer (labeled 4 and 5) of the first double layer expands at $d=1$ BL, as indicated by the arrow in Fig. 6(a). The space of the substrate double layer also expands at $d=1$ BL. In Fig. 6(c), the space of double layer in the second layer expands at $d=2$ BL, at which the naked area of the second layer becomes maximum and the change of atomic positions should result in the calculated intensity. In Fig. 6(d), the space of the double layer in the third layer also expands at $d=3$ BL. However, the space of the double layer in the fourth layer does not expand and is the same as the substrate, as shown in Fig. 6(e).

In order to show an overall change in the atomic position during growth, it is very useful to examine how the one-beam potential is changed as given in Fig. 7. The numbers indicated in the right-hand side correspond to the mean thickness in BL, i.e., the number 0 indicates the potential of the 7×7 substrate. Even at the small amount of $d=0.5$ BL, the potential is altered by the growth of the first and second layers on the substrate, as indicated by 0.5 in Fig. 7. The space of the first double layer starts to expand at $d=0.5$ BL and reaches the maximum at $d=1$ BL. Since the thickness showing the maximum alternation coincides with that showing the maximum naked area of the first layer, we can identify that the structure model represents the real structure of the first growing layer. The lower layer of the first double layer is formed at low position (arrow 1) compared with the ideal position indicated by a dotted line. With this decline of the lower layer of the first double layer (arrow 1), the upper layer of the substrate double layer (arrowhead 0) is

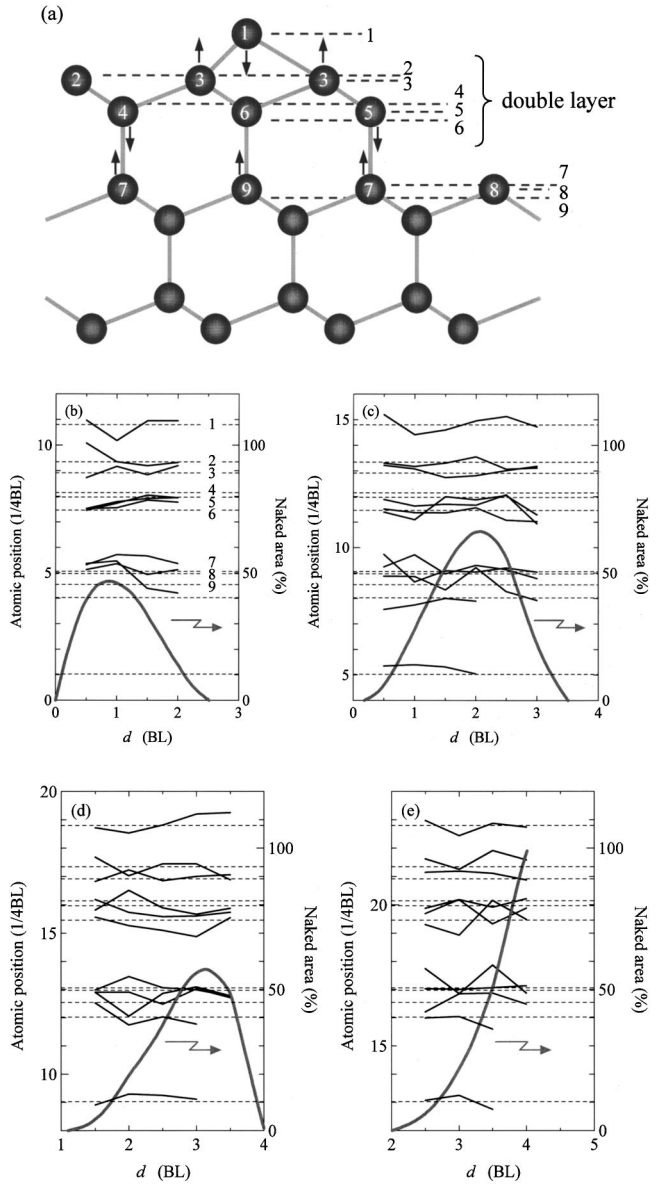

FIG. 6. Optimized atomic positions in the DAS structure at each growing layer as a function of mean thickness *d*. (a) A model of the first growing layer showing the notation of each atomic position. The changes of atomic position in the first, second, third, and fourth layer are plotted in (b), (c), (d), and (e), respectively. In the lower part of each figure, the change in the naked area is also plotted by a thick line.

pulled up. In the similar way, with the decline of the lower layer of the second double layer (arrow 2), the upper layer of the first double layer (arrowhead 1) is pulled up at $d=2$ BL. At $d=3$ BL, with the decline of the lower layer of the third double layer (arrow 3), the upper layer of the second double layer (arrowhead 2) is also pulled up. However, at $d=4$ BL, both the upper layer of the third double layer (arrowhead 3) and the lower layer of the fourth double layer (arrow 4) do not change and these spaces are the same space as the substrate. From these results, the double layer of growing layer systematically changes during the growth up to $d=3$ BL.

We should note that the expansion of these double layers relates to the growth mode. In other words, the expansion is

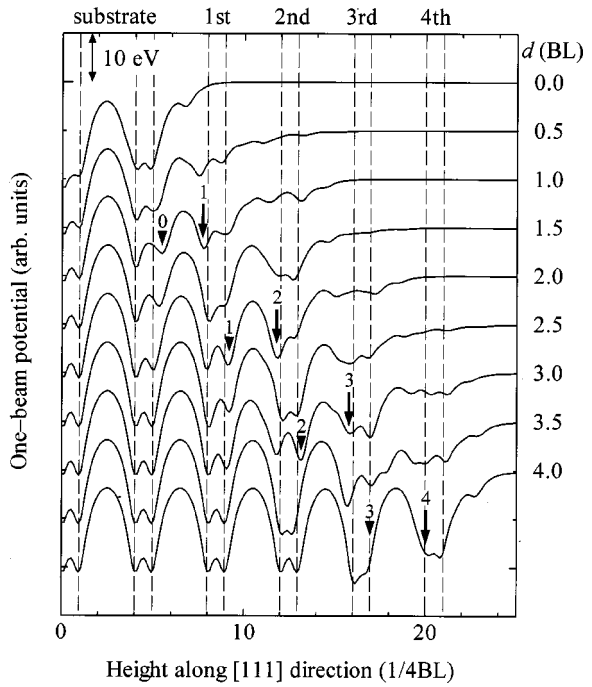

FIG. 7. Changes in the one-beam potential during each growth stage. The vertical dashed lines indicate the ideal positions of the double layer. A curve at $d=0.0$ BL indicates the potential of the substrate.

measured only when the 3D islands are grown on the substrate at $d<3$ BL. Moreover, we note that the space of the substrate double layer intensely expands at $0.5<d<2.0$ BL, at which the Bragg peaks strongly broaden in the experiment. Therefore the broadening is caused by the expansion of only the substrate double layer. When the nucleation and growth of Si islands progresses on the substrate surface, the atoms constructing the 7×7 DAS structure in the substrate must be rearranged. Therefore it is considered that the broadening of Bragg peaks at the initial growth relates to the intermediate structure in the rearrangement process of DAS structure on the substrate surface.

We consider that the expansion of the space in the double layer does not spread to the whole layer but localizes in the vicinity of the island edge. In 3D island growth, since the islands are composed of multilayers, the edge occupies a large part on the surface compared with the Si layer formed by the layer-by-layer growth. Unfortunately we cannot confirm this view, because the one-beam potential gives only an average value in a plane parallel to the surface. To confirm this view, we are going to measure RHEED rocking curves at a certain incident condition and to analyze this by using a many-beam calculation. From the analysis, we will be able to clarify in the near future the intermediate structure during the growth of 3D islands on the Si(111)-7×7 surface.

It is expected that the double layer structure changes after growth. Then, we are studying the change of the expanded double layer after the growth.

V. SUMMARY

We have measured RHEED rocking curves continuously during homoepitaxial growth on the Si(111) surface at $T_s=380\,^{\circ}$C. The features of the measured rocking curves are as follows: (1) The peak at $\theta=1.3^{\circ}$ shifts to lower glancing angle and subsequently disappears at $d\approx2$ BL; (2) The peak at $\theta=1.8^{\circ}$ appears at $d\approx0.4$ BL, and gradually shifts to lower angle with growth; (3) In further growth, these peaks construct one peak at $\theta=1.3^{\circ}$ with a growth of $d=3$ BL; (4) For notable features, the width of the 333, 444, and 555 Bragg peaks becomes broad with growth, and subsequently becomes sharp at $d=3$ BL. The change in the rocking curve during growth can be explained by considering that the space of the double layer in the (111) plane of the multilayer islands expands at the initial growth stage, and the space of the double layer is restored to the normal spacing after the layer-by-layer growth starts. Moreover, it is considered that the broadening of Bragg peaks at the initial growth relates to the rearrangement process of stable DAS structure on the substrate surface.

ACKNOWLEDGMENTS

This work was partly supported by Takahashi Industrial and Economic Research Foundation and the Grants in Support of the Promotion of Research at Yokohama City University.

*Author to whom all correspondence should be addressed. Electronic address: shigeta@yokohama-cu.ac.jp

[1] Y. Shigeta and K. Maki, Jpn. J. Appl. Phys., Part 1 **29**, 2092 (1990).
[2] Y. Shigeta, J. Endo, and K. Maki, Phys. Rev. B **51**, 2021 (1995).
[3] Y. Shigeta, J. Endo, and K. Maki, J. Cryst. Growth **166**, 617 (1996).
[4] Y. Shigeta, Surf. Rev. Lett. **5**, 865 (1998).
[5] Y. Shigeta, H. Fujino, and K. Maki, J. Appl. Phys. **86**, 881 (1999).
[6] D. J. Eaglesham, H.-J. Gossmann, and M. Cerullo, Phys. Rev. Lett. **65**, 1227 (1990).
[7] D. L. Smith, C. Chen, G. B. Anderson, and S. B. Hagstrom, Appl. Phys. Lett. **62**, 570 (1993).
[8] K. Takayanagi, Y. Tanishiro, S. Takahashi, and M. Takahashi, Surf. Sci. **164**, 367 (1985).
[9] K. Yamaguchi, H. Mitsui, and Y. Shigeta, J. Vac. Sci. Technol. A **15**, 2569 (1997); *ibid.* **17**, 3530 (1999).
[10] Y. Shigeta, Y. Fukaya, H. Mitsui, and K. Nakamura, Surf. Sci. **402–404**, 313 (1998).
[11] M. Ichikawa and T. Doi, Appl. Phys. Lett. **50**, 1141 (1987).
[12] A. Ichimiya, Jpn. J. Appl. Phys., Part 1 **22**, 176 (1983).
[13] A. Ichimiya, *The Structure of Surfaces III*, Springer Series in Surface Sciences Vol. 24 (Springer, Berlin, 1991), p. 162.
[14] D. W. Marquardt, J. Soc. Ind. Appl. Math. **11**, 431 (1963).
[15] M. R. Osborne, J. Aust. Math. Soc. B, Appl. Math. **19**, 343 (1976).
[16] A. Ichimiya, Surf. Sci. Lett. **192**, L893 (1987).